DESIGN OF PULSED HIGH-VOLTAGE POWER FOR ELECTROSTATIC PRECIPITATOR

L.J. FAN[†‡], X.C. PAN[†], Z.X. HUANG[†], and X.D. ZU[†]

† ZNDY, School of Mechanical Engineering, Nanjing University of Science and Technology, Nanjing 210094, Jiangsu, China.
‡ Anhui Special equipment inspection institute, Hefei 230000, Anhui, China.
E-mail:pxc_nust@163.com

***Abstract*—In this paper, the physical model of anti-corona phenomenon was established, the theoretical model of anti-corona suppression powered by an electrostatic precipitator (ESP) pulse has been obtained. A dust collecting method was suggested in which a gas has ionized by an electrostatic field to adsorb dust particles to an electrode. The relationship between pulse frequency, amplitude pulse width and dust removal efficiency were tested. Research results showed that the physical model of anti-corona phenomenon could reflect the process of corona generation. The circuit scheme of superimposing high-voltage pulse based on direct current high voltage can effectively suppress the anti-corona phenomenon and improve the dust removal efficiency.**

***Keywords*—Electrostatic precipitator (ESP); High-voltage pulse; Anti-corona phenomenon; Flashover; Resonant pulse generation.**

I. INTRODUCTION

Early electric dust removal direct current (DC) high voltage power of supply scheme has been widely used due to the simple structure (Grass *et al.*, 2004). In a factory environment, when the high specific resistance dusts enter the strong electric field and reach the positive dust-collecting electrode, it is difficult for the high specific resistance dust to release its own negative charges (Bazan *et al.*, 2017). As more and more dust arriving at the dust collecting plate, a negative dust layer which is adsorbed on the dust collecting plate and is not easily removed by the rapping device forms, become an anti-corona phenomenon.

It causes the current of the corona rapidly increase, accompanied by the spark discharge, making the high-voltage supply current fluctuate continuously, reducing the efficiency of the dust collector, and even leading to dust collector failure and damage (Yanallah *et al.*, 2012; Liu *et al.*, 2004).

When a high-voltage pulse is superimposed on the DC high voltage, the pulse width of high-pressure is small、the actuation duration of high-voltage is short, which makes the breakdown voltage of the electric field higher compared to the DC (Tang mingkang, 2010). Meanwhile, the average electric field corona voltage and corona current is reduced. It effectively inhibits the anti-corona phenomenon, and the dust removal efficiency is improved. In addition, it will not generate a secondary dust. In this way, the circuit losses have been reduced and the electrostatic precipitator (ESP) performance has been improved (Li *et al.*, 2000).

However, since the physical mechanism of the current anti-corona phenomenon is not yet clear, it is difficult to determine the relationship between the occurrence of the anti-corona phenomenon and the quantitative parameters such as charge and mass of the charged dust. The working conditions on the site is also inconsistent, therefore, the electrical parameters are difficult to be universal on the superimposed high-voltage pulse technical solutions. For different conditions and different types of dust, repeated commissioning on site is necessary to achieve the desired effect.

This paper introduces the general law of charged dust movement, describes the formation of anti-corona phenomenon, according to the elimination of anti-halation phenomenon. This paper presents an anti-corona phenomenon physical model, combining the physical model; a counter-corona phenomenon has developed to eliminate the pulse power supply. Then the design and simulation of the main circuit has been carried out (Fríes *et al.*, 2017). Considering the dust removal efficiency and the probability of anti-corona phenomenon, the 200Hz pulse frequency, the 48kV pulse voltage amplitude and the 30kV stack DC voltage amplitude have been selected as the optimal environmental ESP operating parameters (Klippel, 2000).

The field tests indicate that the technical solution of high-voltage pulse superimposed on the DC high voltage basis can effectively eliminate the anti-corona phenomenon, improves the dust removal efficiency.

The remainder of this paper is organized as follows. Section 2 describes the general rule of charged dust movement, Section 3 presents the formation mechanism of anti-corona phenomenon, Section 4 describes the system design and principle analysis, Section 5 gives the experimental results and analysis, followed by the conclusion.

II. THE GENERAL RULE OF CHARGED DUST MOVEMENT

In general, most of the particle size of airborne dust particles is 0.1-10 μm. Dust particles with a particle size of less than 0.1μm behave like molecules and collide with each other to create an irregular Brownian motion. When the dust is in the electric field of the precipitator, the ionized electrons of the gas continuously collide with the dust particles, and then the dust will get charged (Yin *et al.*, 2009). The equilibrium charge expression is:

$$Q_n = \pi\varepsilon_0\left[1+2\left(\frac{\varepsilon_r-1}{\varepsilon_r+2}\right)\right]E_r d_D^2 \quad (1)$$

where Q_n is the equilibrium charge ; E_r is the electric field strength ; d_D is the particle diameter ; ε_0 is the dielectric constant of vacuum ; ε_r is the relative dielectric constant of air.

Charged dust particles will move to the positively charged dust collection plate, dust layer's discharging expression is:

$$Q = Q_0 \exp\left(-\frac{t}{\rho_t\varepsilon_0\varepsilon_p}\right) \quad (2)$$

where ρ_t is the specific resistance of the dust (that is, the resistance per unit volume), ε_0 is the dielectric constant of vacuum, ε_p is the dielectric relative permittivity, Q_0 is the discharge capacity of the first layer.

Several conclusions can be drawn from Eq. (1) and Eq. (2):

Firstly, The greater the specific resistance of dust, the longer the discharging time;

Secondly, there is no time factor in Eq. (1) compared to Eq. (2), so it can be assumed that the dust is charged so fast that the charging time can be neglected.

Meanwhile, it is assumed that the charge (charged dust) in the electric field space of the precipitator is unrestricted. Since the discharging speed of the dust is far greater than the charging speed, a potential barrier will be formed (Yin *et al.*, 2009).

Obviously, the formation of the potential barrier will affect the behavior of charged dust, leading to charged dust cluster and oscillation. Therefore, it is necessary to analysis the impact of formation of the potential barrier on the charged dust's behavior between electrodes

In order to derive the time behavior of charged dust, we consider an infinitely thin round electric charge layer with radius of a, and its density is $-\rho$. It lies between two infinite parallel conductor walls, as shown in Fig. 1.

The impact of gravity on charged dust and the collision caused by the thermal movement between dusts are neglected.

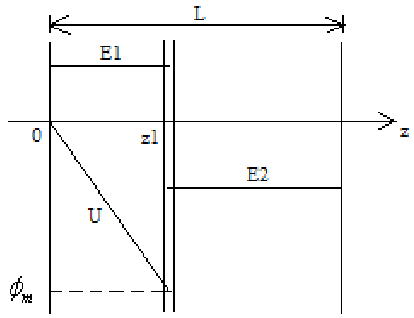

Figure 1. An infinitely thin charge layer model located between parallel conductor walls.

Assuming that the charge of the charged dust layer is $-\rho$, the electric field of the two regions can be expressed as follows.

$$\vec{E} = \frac{\vec{e}_z\rho}{2\varepsilon}\left(1-\frac{z}{\sqrt{z^2+a^2}}\right) \; 0 \le z < z_1 \quad (3)$$

And

$$\vec{E} = \frac{-\vec{e}_z\rho}{2\varepsilon}\left(1+\frac{z}{\sqrt{z^2+a^2}}\right) z_1 \le z \le L \quad (4)$$

where M is the charge layer mass per unit area, considering the one-dimensional case, the area of the charge layer is large enough and moving only along the Z-axis (a»z), then the non-relativistic equation of motion of the charge layer, charged by ρ_1, at $z_1 \le z \le L$ is:

$$\frac{d^2z}{dt^2} = \frac{\rho_1\rho}{2\varepsilon M}\left(1+\frac{z}{a}\right) \quad (5)$$

The solution of the equation using the initial conditions and the boundary conditions is:

$$z = \frac{L}{2}(1-\cosh\omega t) + \frac{V_0}{\omega}\sinh\omega t \quad (6)$$

where V_0 is the initial velocity of the charge layer, ω is given by:

$$\omega^2 = \frac{\rho\rho_1}{2\varepsilon aML} \quad (7)$$

It can be seen that the movement of the thin charge layer is related to ω, and ω is related to the mass of charged dust, the amount of charge etc. Meanwhile, we can see from (6) that, when $\frac{V_0}{\omega} = \frac{L}{2}$, even if t approaches infinity, there exists a nonzero limit $L/2$ for the motion trajectory Z of the charge layer, indicating that the charge layer is reflecting at this time, clusters and oscillations of charged dust will be formed so that it cannot reach the anode.

It should be noted that, this research emphases on the single electric charge layer and its movement behavior. The time behavior of the charge layer formed by the aggregation of charged dust is extremely complicated, and the charge layer models neglect it. In the electrode gap, there are multiple charge layers due to the aggregation of the charged dust particles. Therefore, the value of ω is dynamically changed due to the coherence between the charge layers, so that it is possible to form a current oscillation or voltage flashover (Keping *et al.*, 2015).

III. FORMATION OF ANTI-CORONA PHENOMENON

The specific resistance of dust can be divided into low specific resistance and high specific resistance. The low specific resistance has high conductivity, so it is easy to release the charge at the dust-collecting electrode. However, the dust characteristic of high specific resistance is opposite. The first layer of high specific resistance has not yet release the charge, according to the previous analysis. Due to the space charge effect, the high resistance of the next layer is difficult to release due to blocking of the first dust collector and the dust has piled up and reflected intermittently to form a surface potential. It is also found that the higher of the specific resistance of the dust, the higher of the surface potential.

The accumulation and oscillation of the dust layer will generate an additional electric field in the dust removal electric field (Yao *et al.*, 2009). It will weaken even shield the electric field of the dust removal, resulting in increased oscillation of the dust particle movement and a decrease in the average driving speed. Eventually, the additional electric field strength will reach the threshold that ionizes the gas in the dust layer gap; the dust layer will be insulation punctured by the insulation and releases a large amount of positive ions toward the corona electrode, which is an anti-corona discharge, cause damage by the anti-corona. Anti-corona onset needs to satisfy the following conditions：

$$E = \rho_t \cdot J \geq E_{\mathrm{cr}} \qquad (9)$$

where E is the field strength of the dust layer; ρ_t is the specific resistance of the dust; J is the current density of the dust layer; E_{cr} is the breakdown electric field strength of the air gap of the dust layer.

The time constant T_d for the release charge of the dust layer has given by (10)

$$T_d = \mathrm{RC} = 8.85 \times \varepsilon_s \times \rho_t \times 10^{-14}(s) \qquad (10)$$

where ρ_t is the specific resistance of the dust is layer; $\varepsilon_{\mathrm{s}} \approx 3$ is the dust layer dielectric constant.

The supply current density of conventional dust removal equipment is about $J = 0.1 \sim 0.5mA/m^2$, breakdown electric field strength of dust layer is about 8-12kV/cm . Substituting the data into the formula (9):

$$\rho_t > \frac{E_{cr}}{J} = \frac{10kV/cm}{(0.1 \sim 0.5)mA/m^2} = (2 \sim 10) \times 10^{11} \Omega \bullet cm \qquad (11)$$

If the specific resistance of the dust is $\rho_t = 2 \times 10^{11}\mathrm{cm} \cdot \Omega$, according to Eq. (10), the discharge time constant of the dust layer is $T_d \approx 0.054s = 54\mathrm{ms}$. The silicon rectifier transformer rectifies all the DC of existing power supply of dust remover and the charging time of the power supply is about 10ms, which is less than the time constant of the dust layer. As a result, only a very small portion of the charge on the surface of the dust layer has discharged at the next power charging. In this way, the surface of the dust layer cannot discharge. With the power supply repeatedly charged, the potential continues to rise, and finally reaches the breakdown electric field strength, the phenomenon of anti-corona happens. Actually, this kind of phenomenon cab be observed when

$$\rho_t > 5 \times 10^{10} cm \bullet \Omega \, .$$

In summary, to eliminate the anti-corona phenomenon, the only way is to make the charging cycle of the power supply less than T_d. Meanwhile, the surface of the dust layer needs the discharge circuit and sufficient time to discharge, that is, high frequency of the power supply waveform equivalent, small duty cycle, so that there will not be much accumulation of charge on the dust layer, inhibiting the generation of anti-corona. The pulse power supply can adjust the charging cycle (pulse width) of the pulse power making it much smaller than the time constant of the dust layer, the charged dust can have enough time to discharge through the circuit shown in Fig. 3. Therefore, when the specific resistance of the dust is high, the pulse power supply can suppress the anti-corona well.

IV.SYSTEM DESIGN AND PRINCIPLE ANALYSIS

A. Design of the power main circuit

Pulsed power superposition scheme is shown in Fig. 2, the DC basic voltage-U_{dc} applied to the electrostatic precipitator body, L_{dc} is the isolated inductance, reducing the impact of pulsed power supply on the DC source, C_{c} is the pulse coupling circuit output capacitor, it is used to achieve DC superimposed on the high-pressure pulse (Jiang *et al.*, 2013). Pulse generating circuit's power is provided by the front-end DC voltage $+U_{ps}$. Inductance L_{ps}, resistance R_{ps}, storage capacitor C_{s} and high-voltage transformer compose the charging path. When the VT switch is closed, the primary side of C_{s} and PT forms a closed path through VT. The leakage inductance of the transformer in the loop, the storage capacitor, and the equivalent capacitance coupled to the primary side of the transformer at the primary side generate series resonance under the excitation of the initial energy of the storage capacitor. Because the resonance will continue to decay, the first resonant pulse will output the maximum pulse amplitude.

When designing the pulse circuit, it is necessary to match the direction of the first resonant pulse with the connection of the DC power source and control the VT disconnect in Fig. 2. A resonant cycle of the loop current completes a sine wave of a complete cycle, and passes to the secondary side of the transformer, through the coupling capacitor C_c superimposed on the electrostatic precipitator body, formes high-voltage pulse in the electrostatic precipitator.

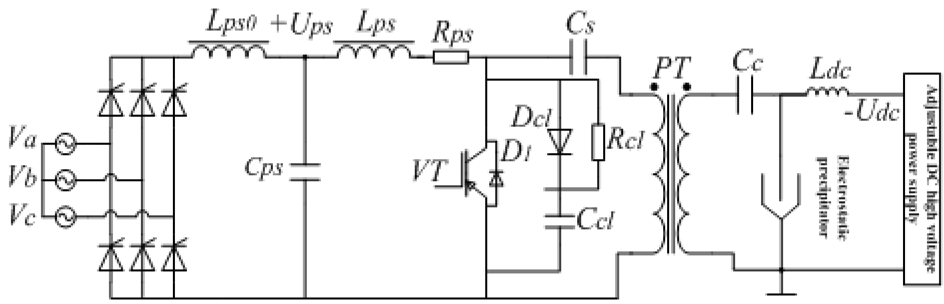

Figure 2. Circuit topology of the pulse power.

B. Circuit theory analysis and simulation

Electrostatic precipitator body is equivalent to a leakage capacitor, represented by R_0 and C_0. In order to facilitate the superposition circuit from the principle, ignoring the auxiliary circuit, regard the high-frequency transformer as an ideal transformer in parallel leakage inductance, and with its approximate equivalent circuit, put the secondary circuit of the transformer coupled to the primary side to analyze and calculate together. Fig. 3 shows the VT turn-on simplified circuit.

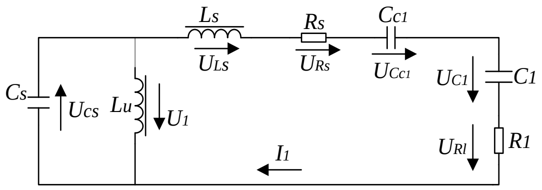

Figure 3. Equivalent RLC series resonant circuit.

The main parameters of the pulse transformer in Fig. 3 are the leakage inductance L_s, the excitation inductance L_u and the equivalent resistance R_s of the winding coil itself. The excitation inductance of the pulse transformer is much larger than the leakage inductance, and the circuit is considered as an open circuit.

The capacitor C_{c1} , the capacitor C_1 and the resistor R_1 are the equivalent parameters converted to the primary side of the transformer secondary circuit.

Set pulse transformer ratio of 1: n, then:

$$R_1 = \frac{1}{n^2}\frac{R_0}{1+\left(\omega C_0 R_0\right)^2};$$

$$C_1 = n^2 \frac{1+\left(\omega C_0 R_0\right)^2}{\omega^2 C_0 R_0{}^2}; \qquad C_{c1} = n^2 C_c$$

Let: $\frac{1}{C} = \frac{1}{C_s} + \frac{1}{C_{c1}} + \frac{1}{C_1}$ (joint capacitance), $R = R_s + R_1$. When $R < 2\sqrt{L_s / C}$, damped oscillation occurs. According to Kirchhoff's Theorem KVL of the circuit, find the voltage drop u_c of the joint capacitance C.

$$u_{c1} = \frac{c}{c_1} U_{ps}\left(e^{-\alpha t}\cos\omega t - 1\right) - \frac{U_{dc}}{n} \tag{12}$$

Pulse generator pulse voltage applied in the precipitator body is the voltage of capacitor C_1 in Fig. 3, according to Eq. (12), the impulse voltage applied to the precipitator body can be calculated:

$$u_{c1} = \frac{c}{c_1} U_{ps}\left(e^{-\alpha t}\cos\omega t - 1\right) - \frac{U_{dc}}{n} \tag{13}$$

In the equation , $\alpha = \sqrt{R/(2L_s)}$; $\theta = \arctan\frac{\omega}{\alpha}$; $\omega = \sqrt{1/\left(CL_s\right) - \left[R/\left(2L_s\right)\right]^2}$ 。

Under the simulation of Phase Inversion Symmetric Method (PISM) software, we set up the HVDC voltage Ups = 21kV, the pulse frequency f = 100Hz, the pulse width τ=140μs, the capacitance C_c of 0.1μF and the transformer ratio 1:60. The simulation waveforms before and after superposition are shown in Fig. 4 (a) and Fig. 4 (b), which verify the correctness of theoretical analysis.

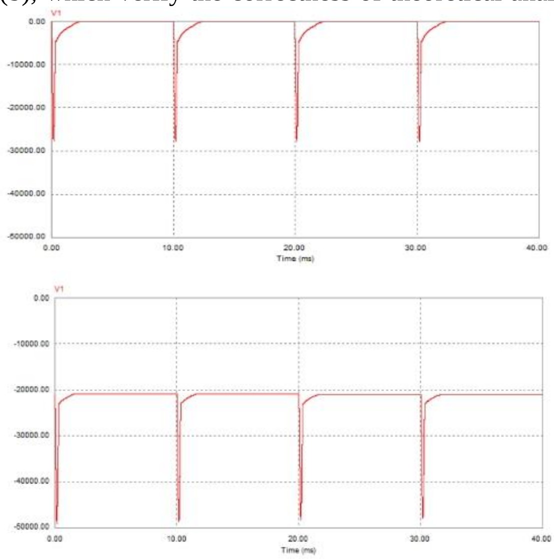

(a) (b)

Figure 4. Simulation waveforms before and after pulse superposition.

V. EXPERIMENTAL RESULTS AND ANALYSIS

According to the previous theoretical analysis and circuit design, an experimental prototype of electrostatic precipitator was set up to complete the commissioning of the circuit, and a field test has been conducted in a steel plant, as shown in Figure 5 (a), (b) below.

(a)

(b)

Figure 5. Test prototype and field test.

Pulse generator circuit debugging set the pulse frequency at 100Hz, pulse width at 50us, measuring the pulse transformer output waveform (high-voltage measurements are measured by 1000 times by the high-pressure probe, high-pressure carbon rod model is Tektronix P6015A)

In the pulse superimposed DC experiment, the high-voltage DC voltage was adjusted to reach 30kV, and then through the host computer to adjust the pulse amplitude to reach 50kV. The analog precipitator load of voltage waveform as shown in Figure 6 below.

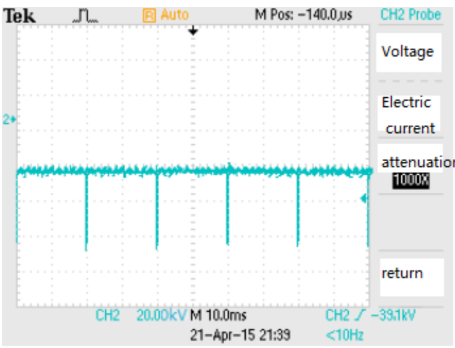

Figure 6. The waveform diagram of loads.

In the field test, the existing dust remover equipment of a steel mill had operating parameters of DC voltage of 45 kV, inlet dust concentration of 1.3g/m^3, outlet dust concentration of 65.36mg/m^3 and dust removal efficiency of 95.01 %. For the designed prototype, a series of pulse voltage and pulse frequency was chosen for the trial operation, and the best operation pulse amplitude and frequency was achieved. Voltage test has been carried out at 150Hz pulse frequency, and the experimental data of dust removal efficiency has been obtained. Its smooth curve can be seen in Figure 7. There is an extreme point of the dust removal of efficiency curve between 47kV and 49kV, so a test with the pulse amplitude of 48kV has been added. The data is as follows: the dust concentration of the inlet is 1.29g/m^3, the dust concentration of the outlet is 17.31mg/m^3, dust removal efficiency is 98.66%. The greater pulse voltage is not conducive to improving the efficiency of dust removal, but exist a peak, so 48kV has chosen as the pulse voltage amplitude set in the followed tests.

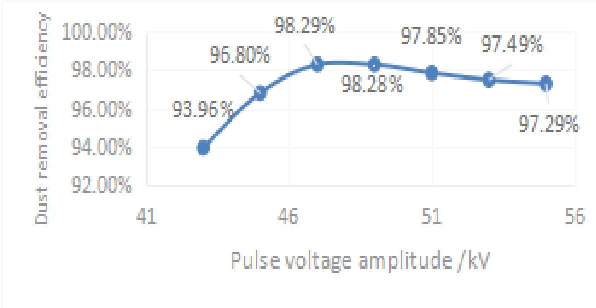

Figure 7. Relationship between pulse amplitude and dust removal efficiency.

Referring to the pulse amplitude of the impact experiments, 48kV pulse voltage was chosen to do the experiments of impulse frequency effects. Fig. 8 shows that as the frequency increases from 140Hz, the dust removal efficiency will gradually increase. After 210Hz, the dust removal efficiency will be gradually reduced, but slower. When the frequency is even higher, dust efficiency dropped sharply. This process shows that the electric field has a saturated charge state, and when the pulse frequency is too high, it will increase the probability of anti-corona electrostatic precipitator phenomenon.

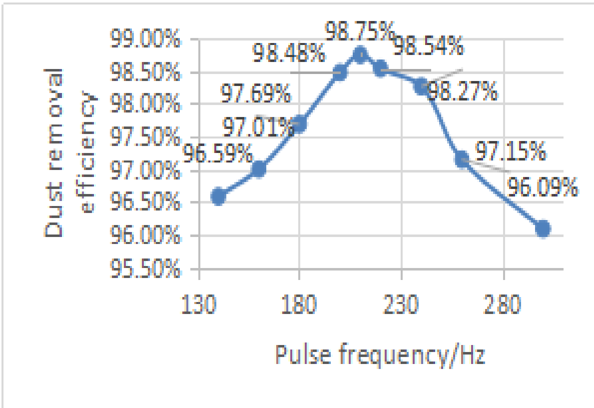

Figure 8. Relationship between pulse frequency and dust removal efficiency.

Voltage flashover can reflect the stability of the electric field within the precipitator, anti-corona occurs generally accompanied by a larger voltage flashover, performing as voltage fluctuations. Through the power control room of monitoring screen every 3 seconds to record a voltage reading, 151 data have been recorded in total and the results have plotted. For comparison, experimental results of 48 kV and 140 Hz superimposed pulsed high voltages were also recorded and plotted in Figure 9, in which U (a) and U (b) shows the voltage flashover waveform before and after superimposition, respectively.

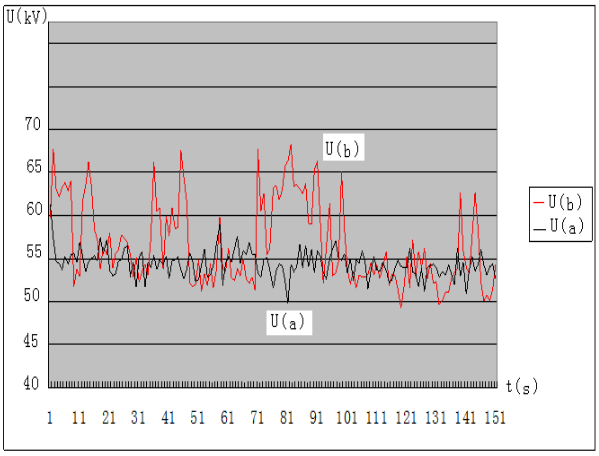

Figure. 9. Superimposed pulse before and after flashover changes.

It is shown that the superimposed high voltage pulse and the voltage flashover ere significantly improved, indicating that anti-corona phenomenon has been effectively suppressed.

In summary, taking the dust removal efficiency and the anti-corona phenomenon probability occurrence into account, select the pulse frequency of 200Hz, the pulse voltage amplitude of 48kV, DC voltage amplitude of 30kV stack as the best environmental ESP operating parameters.

VI. CONCLUSIONS

This paper proposes a direction for suppressing anti-corona and a reverse corona phenomenon that eliminates the pulse power supply. Field tests showed that the technical solution of high-voltage pulse superimposed on DC high voltage can effectively eliminate the anti-corona phenomenon and improve the dust removal efficiency. It will become a reference to the promotion of high-voltage pulse power in the field of electric dust removal.

ACKNOWLEDGEMENTS

This work was supported by the National Natural Science Foundation of China (Grant Nos. 11502118).

REFERENCES

Bazan, V., E. Brandaleze and P. Sarquis, “Evaluation of the use of slag from the mining of Au and Ag as a replacement of the sand in Ccment mortars”, *Latin American Applied Research*, **47(2)**, 77-82 (2017).

Fríes, E. R., M.E. Berli, S. Ubal, D. M. Campana, and J.D. Paolo, “Computer simulation of platelet activation in a pulsatile ventricular assist device, through finite elements and a simplified geometry”, *Latin American Applied Research*, **47(3)**, 83-88 (2017).

Grass, N., W. Hartmann and M. Klockner, “Application of different types of high-voltage supplies on industrial electrostatic precipitators”, *IEEE Transactions on Industry Applications*, **40(6)**, 1513-1520 (2004).

Jiang, Y.F., L.Y. Li, Y.J. Xie, “Research on pulse high voltage power supply for ESP[C], *Proceedings of 15th Conference of ESP*, Bengbu, **1(1)**, 271-275 (2013).

Keping, Y.A.N., L.I. Shuran, F.E.N.G. Weiqiang, Q. Zhen, *et al.*, “Analysis and prospect on key technology of high-voltage discharge for environmental engineering study and application”. *High Voltage Engineering*, **41(8)**, 2528-2544 (2015).

Klippel, N., “The influence of high-voltage pulse parameters on corona current in electrostatic precipitators”, *Journal of Electrostatics*, **49(1-2)**, 31-49 (2000).

Li, J. W., Z.M. Xiong and X.H. Jiang, “Removing dust technique study on high pressure impulse electro precipitator”, *Environmental Protection Science*, **26(99)**, 1-3 (2000).

Liu, S.T., M.Y. Hu, L.F. Li, S. Zhang, and X. Han, “Simulative Experimental Study on Back Corona of Electrostatic Precipitator”, *Industrial Safety and Environmental Protection*, **30(10)**, 21-23 (2004).

Yanallah, K., and F.A. Pontiga, “A semi-analytical stationary model of a point-to-plane corona discharge”, *Plasma Sources Science and Technology*, **21(4)**, 045007 (2012).

Yao, Q., S.Q. Li, H.W. Xu, J.K. Zhuo, Q. Song, “Studies on formation and control of combustion particulate matter in China. A review”, *Energy*, **34(9)**, 1296-1309 (2009).

Yin, L.Q. and J. Wang, “Study on the influences and improvement measures of dust resistivity to electrostatic precipitator”, *Electric Power Environment Protection*, **5(1)**, 34-37 (2009).

Received: December 15th 2017
Accepted: June 30th 2018
Recommended by Guest Editor
Juan Luis García Guirao